



On the importance of accurate pole and station coordinates for VLBI Intensive baselines

Lisa Kern¹ · Matthias Schartner² · Johannes Böhm¹ · Sigrid Böhm¹ · Axel Nothnagel¹ · Benedikt Soja²

Received: 14 April 2022 / Accepted: 7 October 2023 / Published online: 1 November 2023
© The Author(s) 2023

Abstract

Very long baseline interferometry (VLBI) is a geodetic technique capable of deriving the complete set of Earth orientation parameters, including the highly variable Earth's phase of rotation. This observable can be expressed through UT1–UTC, the difference between the Universal Time and the Coordinated Universal Time. The so-called *Intensive* sessions, or *Intensives*, are typically 1-h sessions between two to three stations that are observed daily with the primary goal of determining UT1–UTC with a short latency. In this publication, we examine the impact of erroneous a priori information on the UT1–UTC estimation with VLBI *Intensive* sessions in a systematic way and on a global scale. Our findings are based on a simulation study which is carried out on a regular 10×10 degree grid of artificial telescopes. In the simulations, realistic errors are introduced in the station coordinates, polar motion and nutation to get a global picture of the impact of these errors on the estimation of UT1–UTC. Our results reveal that in contrast to errors in the horizontal components of the station coordinates, an error in the station height only slightly affects the UT1–UTC estimate. North–south-oriented baselines are in general strongly affected by errors in the a priori information. In all cases, very short and very long baselines as well as baselines with a midpoint close to the equatorial plane are less robust. On the other hand, east–west-oriented baselines, except equatorial baselines, seem to be rather resistant against errors of these a priori values.

Keywords VLBI · Intensives · UT1–UTC · Simulation

1 Introduction

The main purposes of geodetic and astrometric very long baseline interferometry (VLBI) observations and analyses include the realization of the International Terrestrial Reference Frame (ITRF) (Altamimi et al. 2016) and the International Celestial Reference Frame (ICRF) (Charlot et al. 2020), as well as the estimation of the complete set of Earth orientation parameters (EOP) (Petit and Luzum 2010). In particular, VLBI is the primary technique for observing the difference between the Universal Time (UT1) and the Coordinated Universal Time (UTC). By observing regular 24-h VLBI sessions with a global network, e.g., IVS (International VLBI Service for Geodesy and Astrometry (Nothnagel et al.

2017)) R1/R4 sessions, all the above-listed parameters can be determined with a latency of around 14 days. The so-called *Intensives* are observed on a daily basis with the exclusive goal of determining UT1–UTC. These 1-h VLBI sessions usually include two to three stations and are therefore highly restricted in the number of observations. Due to the reduced geometry of VLBI *Intensive* sessions, only a few parameters besides the main parameter of interest can be derived compared to regular 24-h sessions, including zenith wet delays per station and a linear function for the clock differences. Thus, the remaining EOP and further the station and source coordinates are fixed to their a priori values. In this way, the accuracy of the UT1–UTC *Intensive* estimates becomes strongly dependent on the accuracy of the a priori information and the overall scheduling process, including the observing geometry. This is the topic which we address in this publication.

In comparison with regular 24-h sessions, *Intensive* sessions have a much shorter turnaround time for product delivery of around one to two days and therefore enable us to regularly monitor this highly variable parameter UT1–UTC.

✉ Lisa Kern
lisa.kern@tuwien.ac.at

¹ Department of Geodesy and Geoinformation, TU Wien, Wiedner Hauptstrasse 8, 1040 Vienna, Austria

² Institute of Geodesy and Photogrammetry, ETH Zürich, Robert-Gnehm-Weg 15, 8093 Zurich, Switzerland

However, due to the limitation in the session duration and participating stations compared to 24-h sessions, the accuracy of UT1–UTC is reduced (between 5 μ s and 20 μ s), making it an important task to improve these short VLBI sessions. In the last decade, various studies have been carried out to improve the accuracy of UT1–UTC *Intensive* observations by analyzing the scheduling algorithm and source selection, increasing the number of observations, or investigating the optimal geometry and orientation concerning these single-baseline sessions. For example, Artz et al. (2012) focused mainly on the increase of the number of observations by introducing 2-h *Intensive* sessions leading to an improvement of the UT1–UTC formal error by a factor of $\sqrt{2}$. Leek et al. (2015) investigated an approach to achieve a higher redundancy which included the usage of twin telescopes and a scheduling algorithm designed to improve the observing geometry. Furthermore, Kareinen et al. (2017) examined the effect of adding a tag-along station to a single-baseline *Intensive* session in a simulation study and observed an improvement of up to 40% in the yearly weighted root mean square error of UT1–UTC. In general, these studies prove that by increasing the number of observations, the UT1–UTC measurement can be improved. However, the amount of recorded data grows, leading to a higher latency.

Other approaches include the improvement of the scheduling algorithm and the source selection. For example, Uunila et al. (2012) showed, based on the findings of Nothnagel and Campbell (1991), that in particular observations in the corners of the mutually visible sky of the participating stations are crucial for the accuracy of UT1–UTC. Furthermore, the impact of the source selection was examined. Later, Baver and Gipson (2014) investigated different source lists as well as the impact of atmospheric turbulence and source loss on the formal errors of UT1–UTC. With the help of a minimization algorithm based on the observation gradient, Gipson and Baver (2015) were able to improve the UT1–UTC observations with VLBI sessions. In their study, they further manifested the importance of corner observations for the geometry stability of the UT1–UTC estimation and examined the effect of using a small set of strong sources instead of all sources. In Baver and Gipson (2020), they continued their study by introducing a newly defined set of sources, called “Balanced 50,” which allowed them to improve the weighted UT1–UTC formal error by 2.6 μ s in comparison with using a source list with all visible sources. A study by Corbin et al. (2020) tried to improve *Intensives* by adjusting the scheduling process by applying a mixed-integer linear programming method to maximize the sky coverage of the selected schedule. Therefore, a newly developed sky coverage score was introduced, leading to an increase in the number of observations and an improvement in the accuracy of UT1–UTC. However, the computation time was increased significantly.

Over the years, many studies focusing on the analysis of the impact of potential errors in the models used in the analysis of *Intensive* sessions have already been performed. Hefty and Gontier (1997) analyzed the sensitivity of UT1 from *Intensives* to inconsistencies in the atmospheric delay model and in the terrestrial and celestial reference frame in the case of the single-baseline session between Wf (Westford, USA) and Wz (Wettzell, Germany). Additionally, several studies (Böhm and Schuh 2007; Böhm et al. 2010; Teke et al. 2015; Nilsson et al. 2017; Landskron and Böhm 2019; Diamantidis et al. 2022; Wang et al. 2022) examined the large impact of missing or inaccurate modeling of the troposphere on the UT1–UTC estimate from *Intensive* sessions and analyzed possibilities to introduce external tropospheric information to improve VLBI *Intensive* sessions.

While Titov (2000) and Malkin (2011) mainly focused on the impact of different nutation models, Nothnagel and Schnell (2008) examined the impact of errors in the a priori polar motion and nutation on UT1–UTC determinations of so-called INT1 and INT2 *Intensive* sessions, organized by the IVS. At the time of the study, single-baseline sessions between Wz and Kk (Kokee, USA) were referred to as INT1 sessions and INT2 sessions that were typically observed between Wz and Ts (Tsukuba, Japan). In this case, the INT2 baseline with the bigger north–south extension was more affected by errors in the polar motion and nutation components. In the following studies, Malkin (2013) and Krasna et al. (2015) tested how seasonal variations in the station position impact UT1 from *Intensive* sessions. They found that neglecting these effects leads to time-dependent and systematic errors in UT1, which can exceed 1 μ s.

Recently, the influence of systematic variations in S/X source positions and the actual location of radio emission at VLBI Global Observing System (VGOS) frequency bands due to source–structure effects and core shift on geodetic VLBI results have been investigated by Xu et al. (2021, 2022). Although these effects may introduce another class of systematic errors of UT1 results from *Intensive* sessions, investigating these effects is beyond the scope of this study.

The most recent study by Dieck et al. (2023) investigated the impact of a geologic event (earthquake with epicenter 80 km near VLBI antenna Mk (Mauna Kea, USA) and moment magnitude of 6.9) on UT1–UTC measured by the single-baseline session between Mk and Pt (Pietown, USA). They managed to derive an expected offset of 67.2 μ s by estimating the sensitivity of the UT1–UTC value to changes in station position (12.4 mm absolute displacement of Mk), which is consistent at the 1.14 σ level with the measured offset (75.7 μ s).

The previously mentioned works primarily focused on effects on a few selected baselines, but do often not allow for a general and global interpretation. In our previous study (Schartner et al. 2021), we followed the approach used by

Schartner et al. (2020) and investigated the impact of the baseline geometry and orientation on the performance of *Intensives*. For this purpose, the simulation results of almost 3200 baselines between artificial antennas placed on a regular 10×10 degree grid were analyzed to find the optimal single-baseline geometry for the determination of UT1–UTC. Concerning the geometry and orientation of these single baselines, it has been a widely accepted hypothesis that long east–west baselines provide the best sensitivity for UT1–UTC observations. Schartner et al. (2021) proved that this is only true for certain lengths and orientations. Moreover, they revealed that equatorial baselines with perfect east–west extensions are not that well suited for the determination of UT1–UTC. In contrast, north–south-oriented baselines, if they possess large x/y coordinate extensions, showed reasonable UT1–UTC accuracy as well. The partial derivatives of the group delay τ with respect to UT1–UTC $\frac{\partial \tau}{\partial \text{UT1-UTC}}$ of the individual baselines and the corresponding limitation of the commonly visible sky were used to explain these findings. Hence, it has been shown that baselines with a wide right ascension band of visible sources, resulting in a great variety in the partial derivatives, lead to good results regarding the determination of UT1–UTC.

In this previous study, it was also shown that the accuracy of UT1–UTC strongly depends on the accuracy of the a priori information. However, following the suggestions of Nothnagel and Schnell (2008), the impact of erroneous a priori polar motion on the UT1–UTC measurements on a global scale was only assessed with analytical equations, based on the partial derivatives of the polar motion components with respect to UT1–UTC. In Schartner et al. (2021), we predicted that in particular baselines with very large north–south extensions are most affected by errors in the polar motion a priori data, whereas perfectly east–west-oriented baselines are much more robust.

In addition to our previous findings, this study now focuses on the numerical impact of rigorous error propagation of erroneous a priori polar motion data, nutation and station coordinates applying realistic errors. For this purpose, we use the same experiment setup as in our previous study (see Sect. 2.2). Our goal is to examine under more realistic conditions if the network constellations, which were suggested to be optimal for the determination of UT1–UTC by Schartner et al. (2021), are still among the best ones. Therefore, simulations are carried out for almost 3200 baselines. We introduce errors of 5 mm in the up–down, east–west and north–south direction of the station coordinates as well as errors of $162 \mu\text{s}$ (corresponding to an arc length of 5 mm at the Earth’s equator) to modify the components of the polar motion x_p , y_p and the nutation offsets dX , dY (see Sect. 2.3). An error of 5 mm in all coordinate components has been chosen since it represents a typical accuracy of station coordinate estimates from daily VLBI sessions. In addition, it is possi-

ble to scale the derived impact to any other number due to a quasi-linear relationship.

Compared to studies by, for example, Hefty and Gontier (1997), Nothnagel and Schnell (2008), Malkin (2011, 2013) and Dieck et al. (2023), we analyze the impact of potential errors in the a priori data on a global scale to derive generally valid statements, which can be used to find geometrically optimal (Schartner et al. 2021) and maximally robust *Intensive* baselines. Thus, we do not focus on currently observed baselines or on the explicit and absolute values of the effects, but instead we give an overview of the impact of different errors on individual baseline types, e.g., short versus long baselines, north–south versus east–west-oriented baselines. Section 3 elaborates on these results including their interpretation. Finally, Sect. 4 summarizes the findings.

2 Method

The simulation study aims at investigating the impact of erroneous a priori information, including polar motion, nutation and station coordinates on the performance of UT1–UTC observations with *Intensive* sessions. To this end, schedules of artificial *Intensive* baselines are generated with VieSched++ (Schartner and Böhm 2019) and simulated rigorously using a standard least-squares adjustment implemented in the Vienna VLBI and Satellite Software (VieVS). More details on the least-squares approach and the software VieVS in general can be found in Böhm et al. (2018).

2.1 Scheduling approach

As already mentioned above, in the course of this study, schedules between artificial VLBI antennas are generated using VieSched++ (Schartner and Böhm 2019). Typically, a source list of approximately 300 sources that are well suited for geodetic purposes is used in the scheduling process of VLBI sessions. For this study, a total of 125 equally distributed and frequently observed sources are available during the scheduling. This source list is based on the CONT17 campaign with the addition of some ICRF3 defining sources to fill gaps in the southern hemisphere. The number of available sources is reduced in order to mitigate effects caused by the differences in source selection from schedule to schedule.

Since *Intensives* between so-called VLBI Global Observing System (VGOS) telescopes are investigated (see Sect. 2.2), the observation duration is fixed to 30 s as is the scan length of contemporary VGOS multi-station network sessions. Moreover, since previous studies (Nothnagel and Campbell 1991; Uunila et al. 2012; Gipson and Baver 2015) showed the importance of observations in the corners of the mutually visible sky for the performance of *Intensive* sessions, the corner observation scheduling algorithm implemented in

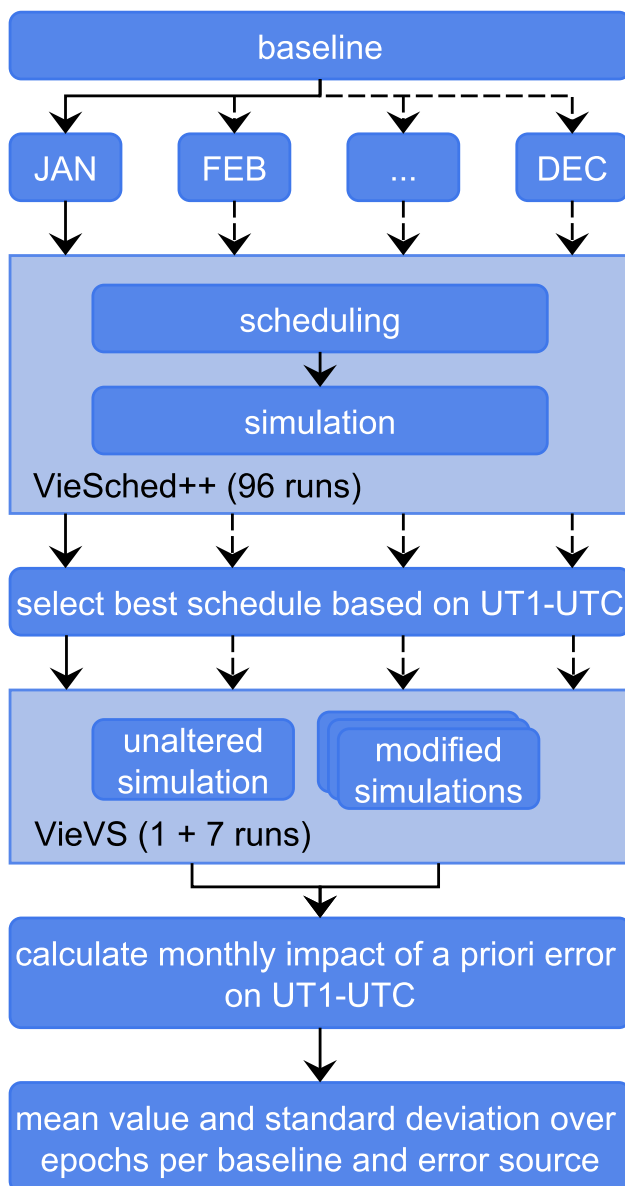


Fig. 1 Flowchart of processing strategy. For the different baselines, monthly schedules are generated using VieSched++ and with the help of simulations, the most promising schedule out of the pool of 96 schedules is selected based on the UT1–UTC precision. In the following, these sessions are simulated again in VieVS while introducing different errors in the a priori values. The impact of the error is quantified as the monthly difference between the UT1–UTC values of the *modified* and *unaltered* evaluation. To make the results comparable, the mean value (bias) and the sample standard deviation of the monthly differences are calculated per baseline and error source

VieSched++ is used (Schartner et al. 2021, Appendix A). The algorithm selects schedules following the standard geodetic scheduling rules (Schartner and Böhm 2019); however, after a certain number n of seconds, the likelihood of observing a source located in a corner of the mutually visible sky is drastically increased. In general, great care was taken to gen-

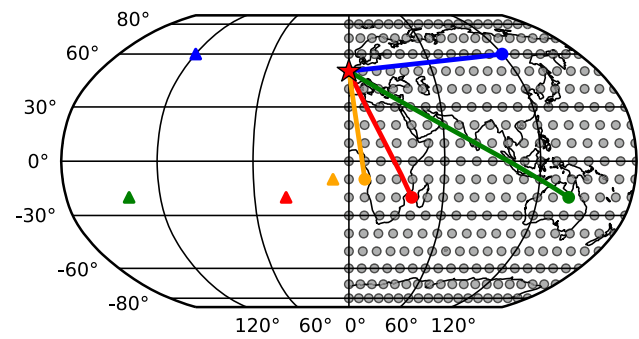


Fig. 2 Sketch of the experiment setup. The red star highlights the reference station. The gray dots highlight positions of the investigated remote stations forming a baseline with the reference station. For illustration purposes, four random baselines are shown using different colors. In the following, simulation results will be displayed at the location of the remote stations. The right-hand side depicts the bias $m(\text{UT1-UTC})$ in UT1–UTC while the corresponding sample standard deviation $\sigma(\text{UT1-UTC})$ is depicted on the left-hand side (e.g., $\sigma(\text{UT1-UTC})$ of the four highlighted baselines is depicted at the location of the colored triangles)

erate schedules of high quality to mitigate scheduling-related effects.

For every session analyzed in this study, a total of 96 different schedules are generated using different optimization strategies. From this pool of schedules, the most promising is selected based on simulations of the expected UT1–UTC precision, see Fig. 1. This schedule is then further processed in VieVS as discussed in Sect. 2.3. Furthermore, per analyzed *Intensive* baseline, twelve monthly schedules of 1-h sessions distributed over one year are generated, starting at 07:00 UTC on the first day of each month. By combining the results of those monthly schedules, i.e., calculating the mean value and sample standard deviation, more robust results can be derived since potential scheduling-related effects, as well as effects caused by source visibility are better averaged out. Initial tests using weekly schedules instead of monthly schedules lead to the same conclusions. Thus, it is not necessary to increase the frequency of the investigated sessions.

2.2 Experiment setup

To analyze the impact of erroneous a priori information on *Intensives*, a regular 10×10 degree grid of artificial VGOS antennas is generated. The grid spans latitudes (lat) from -80 to $+80$ degrees and differences in longitudes (δlon) from 0 to 180 degrees resulting in 17 latitude levels and 19 longitude levels and 323 artificial antennas (see Fig. 2). These artificial antennas have the same properties as the WETTZ13S telescope and can therefore be classified as VGOS antennas (Petrachenko et al. 2012; Niell et al. 2018). The decision to analyze an artificial grid of identical antennas is chosen to properly identify and compare solely the impact of erroneous a priori information. In the case of analyzing real

Intensive baselines, station-dependent effects such as slewing speeds, horizon masks and sensitivities will superimpose these effects.

As already discussed in Schartner et al. (2021), it is sufficient to only examine baselines originating from one reference meridian and baselines within the 19 different longitude levels, due to the fact that the Earth is approximately rotationally symmetric. For this reason, in our investigations, all globally possible baselines are covered by simply rotating the baseline around the z-axis. Here, the reference meridian is always located at zero degrees longitude. Possible differences in the source visibility induced by this simplification are counteracted by the fact that monthly schedules over one year are generated, comprising all possible changes in sidereal time. In the following, only baselines between the reference stations at $lat \geq 0$ and at $lat = -30$ on the reference meridian and any other antenna are investigated making use again of the north–south symmetry. This results in nine reference stations and 322 possible and unambiguous baselines per reference station, leading to a total of almost 3200 investigated baselines. The antennas on the southern hemisphere of the reference meridian are not investigated since, despite the source selection (Plank et al. 2015; Charlot et al. 2020), the performance should be approximately the same as for the baseline mirrored at the equatorial plane. This assumption has been confirmed by investigating one southern reference station at -30 degrees alongside with the nine reference stations located at the northern hemisphere.

In Fig. 2, the experiment setup is illustrated using a reference station at a latitude of 50 degrees, which is highlighted as a red star, whereas the remaining 322 antennas are marked as gray dots. In the background, the coastlines are displayed, but as already mentioned the grid can be rotated around the z-axis resulting in a shift in longitudes without changing the outcome of this study. It is also anticipated here how the obtained results (mean value and standard deviation, see Sect. 2.3) of each baseline are presented in Sect. 3 using four random baselines highlighted in different colors. The mean value regarding one baseline can be found at the location of the corresponding remote station (highlighted as colored dot) and the standard deviation on the left side (highlighted as colored triangle). In Sect. 3, the left and the right sides of each individual plot are color-coded and are bilinearly interpolated to generate a smooth picture.

2.3 Erroneous a priori information

We investigate seven scenarios, where constant errors are introduced in the coordinates of the remote station, as well as in the a priori polar motion and nutation information. It is sufficient to only investigate errors in the coordinates of the remote station since the reference meridian can be shifted to the location of the remote station and the baseline can be

mirrored without changing the outcome of this study. The UT1–UTC values of these seven *modified* evaluations are then compared to the results from an *unaltered* simulation, which refers to a simulation where no errors are introduced. This leads to monthly UT1–UTC differences per baseline representing the impact of the individual errors (see Fig. 1).

Firstly, in separate evaluations, the up, east and north coordinates are modified with an error of 5 mm. Errors in station coordinates can not only stem from wrong a priori information. Instead, they can also be related to un- or mis-modeled deformations of the telescope and loading effects caused by oceans, atmosphere, or hydrology. Moreover, they can be induced by gross errors in the data itself or by missing or inaccurate modeling of the troposphere. In the case of *Intensives*, in general, no tropospheric gradients are estimated due to the highly restricted number of observations and the restricted sky coverage. In previous studies by Böhm and Schuh (2007) and Böhm et al. (2010), the impact of missing or inaccurate modeling of the troposphere has been investigated using the *Intensive* session between Wz and Ts. It was found that neglecting gradients of 1 mm changes the horizontal station position in that direction by about 7 mm, which in turn has an impact on the estimation of UT1–UTC. As a rule of thumb, the change in UT1–UTC is about $15 \mu\text{s}$ per 1 mm sum of east gradients over the two sites. Furthermore, also Gipson and Baver (2016) concluded that gradients have a large effect on the UT1 estimation using *Intensive* sessions and that the accuracy of UT1 can be improved by using the gradient information derived from IVS R1/R4 24-h sessions or by using tropospheric information from Global Navigation Satellite Systems (GNSS) (Teke et al. 2015; Nilsson et al. 2017; Diamantidis et al. 2022; Wang et al. 2022).

Besides that, an error of $162 \mu\text{as}$ (corresponding to an arc length of 5 mm at the Earth's equator) is used to compromise the x_p - and y_p -component of the polar motion as well as the dX - and dY -component of the nutation offsets of the IERS finals EOP series (IAU2000), used as a priori information during the analysis. To create realistic conditions, besides the UT1–UTC offsets, linear clock differences between the stations and tropospheric zenith delay offsets per station are estimated during the least-squares adjustment in VieVS. Moreover, since we are only interested in the differences induced by erroneous a priori information, no additional error sources such as white noise, troposphere, or clock drifts are simulated in the process.

The results of all evaluations consist of a grid of monthly differences in the UT1–UTC value between the *modified* and *unaltered* version per reference station and error source leading to over 270,000 simulated baselines. For the comparison of the baselines, these monthly UT1–UTC differences per baseline are averaged, leading to one UT1–UTC bias $m(\text{UT1–UTC})$, and the sample standard deviation $\sigma(\text{UT1–UTC})$ over the epochs is calculated to represent the impact

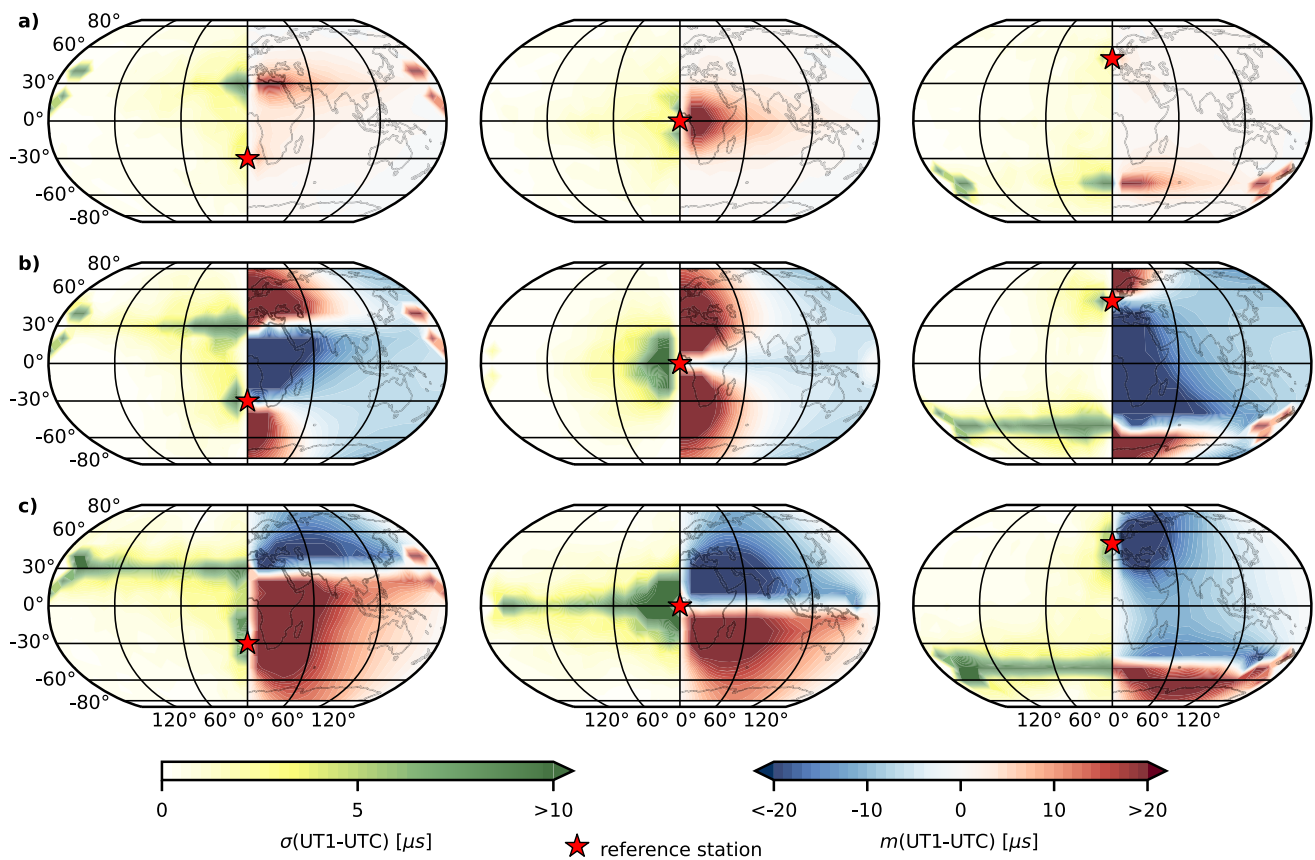


Fig. 3 Impact of erroneous a priori station coordinates on the performance of *Intensive* sessions. Within each subplot, the resulting bias $m(\text{UT1-UTC})$ is depicted on the right while the corresponding standard deviation $\sigma(\text{UT1-UTC})$ is depicted on the left. In the first column, the reference station is located at -30 degrees latitude, in the second

column at 0 degrees and in the third column at 50 degrees. In each row, a different error is introduced in the simulation process, i.e., an error of 5 mm in up (a), east (b) and north direction (c) of the remote station. Bilinear interpolations between the grid cells have been used to generate these plots

of the induced error on the individual baselines (see Fig. 1). The need to calculate and display the sample standard deviation arises from the fact that with symmetric fluctuations in the monthly UT1-UTC differences, regardless of their magnitude, the bias $m(\text{UT1-UTC})$ can become zero, which erroneously symbolizes a robust baseline. For the sake of simplicity, when we refer to the standard deviation in the following, the sample standard deviation is meant.

3 Results

In the following, the simulation results of three representative reference stations at the latitudes of -30 degrees, 0 degrees and 50 degrees are presented. To quantify the global impact of the individual errors, the absolute biases $m(\text{UT1-UTC})$ are compared to the formal errors in UT1-UTC estimates from *Intensive* sessions, which are typically between $5 \mu\text{s}$ and $20 \mu\text{s}$, corresponding to an arc length of 2.3 mm and 9.3 mm at the Earth's equator.

3.1 Errors in station coordinates

In Fig. 3, the topocentric station coordinates of the remote station have been corrupted with an error of 5 mm in the up direction (3a), in the east direction (3b) and in the north direction (3c).

Errors of 5 mm added to the a priori up-component seem to introduce only a small bias in UT1-UTC (small $m(\text{UT1-UTC})$ values). In this first evaluation, only approximately 8% of the baselines exhibit absolute biases $m(\text{UT1-UTC})$ of $> 5 \mu\text{s}$ and 3% of the baselines exhibit biases of $> 20 \mu\text{s}$. Mainly short baselines and baselines with a midpoint close to the equatorial plane, where the condition $lat_1 + lat_2 \approx 0$ is met, are affected.

In contrast, station coordinate errors introduced in the horizontal components result in higher $m(\text{UT1-UTC})$ values. In Fig. 3b, an error of 5 mm is introduced in the east-component of the remote station, while in Fig. 3c, an error of 5 mm is introduced in the north-component. In the case of an error in both horizontal components, the biases $m(\text{UT1-UTC})$ are

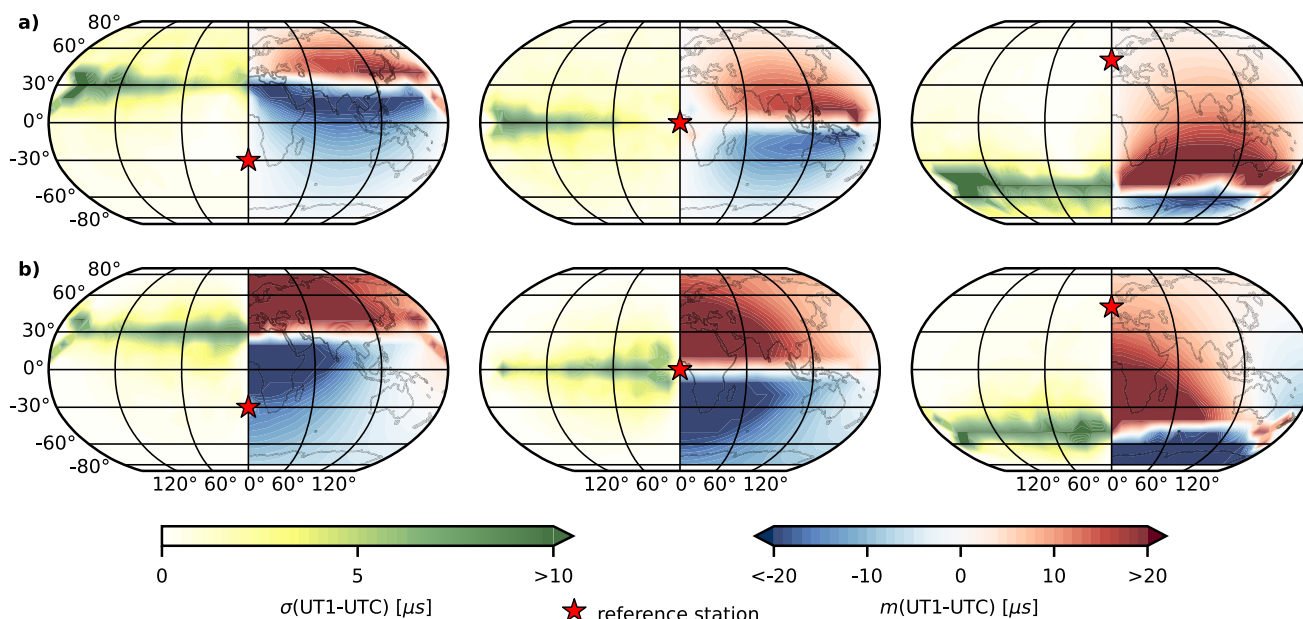


Fig. 4 Impact of erroneous a priori polar motion on the performance of *Intensive* sessions. Within each subplot, the resulting bias $m(UT1-UTC)$ is depicted on the right while the corresponding standard deviation $\sigma(UT1-UTC)$ is depicted on the left. In the first column, the reference station is located at -30 degrees latitude, in the second

column at 0 degrees and in the third column at 50 degrees. In each row, a different error is introduced in the simulation process, i.e., an error of $162 \mu s$ in the x_p - (a) and y_p direction (b) of the polar motion. Bilinear interpolations between the grid cells have been used to generate these plots

clearly above the formal uncertainties of UT1–UTC estimates, since approximately 65–85% of the baselines result in an absolute value of over $5 \mu s$ and 19% of over $20 \mu s$. Overall, long baselines between reference stations and remote stations at low- to mid-latitudes perform the best, i.e., are less affected by errors in the horizontal components. Although baselines with a midpoint close to the equatorial plane and short baselines seem to be less affected by erroneous station coordinates, visible through $m(UT1-UTC)$ values close to zero, one has to be aware that the scatter of the monthly UT1–UTC differences given by the standard deviations $\sigma(UT1-UTC)$ is relatively high, with magnitudes of $10 \mu s$ up to $50 \mu s$. Therefore, they are not resistant against erroneous station coordinates and thus not suitable for UT1–UTC measurements. Moreover, very long baselines between stations with big differences in latitude lead to high $m(UT1-UTC)$ values or no feasible result at all (white areas) due to the lack of observations caused by the highly restricted mutually visible sky. In our previous study (Schartner et al. 2021), based solely on geometry, north–south-oriented baselines between a station on the equator and one near the poles performed only 50% worse compared to the most optimal one and therefore were suggested to be still suitable for UT1–UTC observations. However, if an error is introduced in the east coordinates (see Fig. 3b) in particular baselines oriented in the north–south direction are strongly affected.

Concerning baselines with a reference station in the southern hemisphere, the only difference in the simulation results lies in the sign of the impact, which is switched for a baseline mirrored at the equatorial plane.

3.2 Errors in polar motion

In Fig. 4, the results of the evaluations using erroneous a priori polar motion information x_p - (4a) and y_p direction (4b) are shown. Concerning the polar motion as well as for the a priori nutation offsets, an error of $162 \mu s$ is introduced. In this case, approximately 50% (x_p)/ 70% (y_p) of the baselines result in absolute $m(UT1-UTC)$ values over $5 \mu s$ and approximately 12%/25% over $20 \mu s$.

An error in the x_p - or y_p -component of the a priori polar motion has a strong effect on equatorial baselines and baselines where the midpoint is close to the equatorial plane whereas short baselines seem to be more resistant. However, it seems like only errors in y_p strongly influence north–south-oriented baselines. The reason for this behavior is the position of the reference meridian with respect to the orientation of the coordinate system of the polar motion. If the reference meridian would be located at 90 degrees longitude, the main effect on north–south-oriented baselines would originate from the x_p -component. Other reference longitudes would result in rotations of the x_p/y_p impacts correspondingly. To sum up, north–south-oriented baselines are

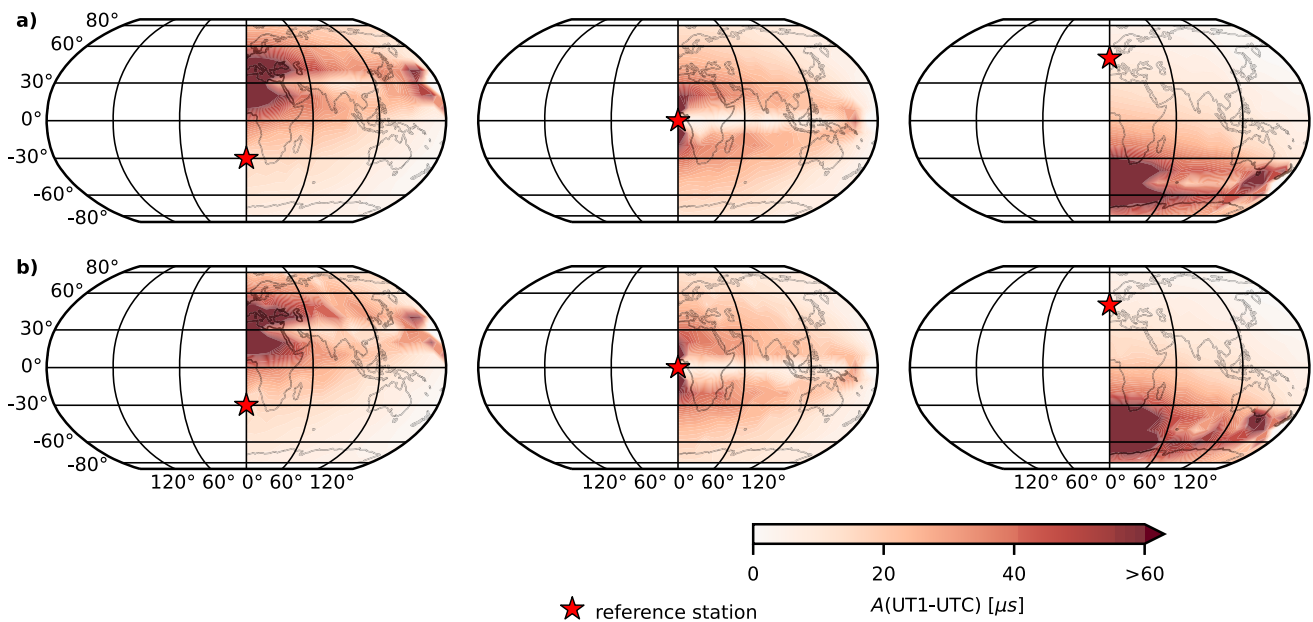


Fig. 5 Impact of erroneous a priori nutation data on the performance of *Intensive* sessions in terms of the amplitude $A(\text{UT1-UTC})$ of the sinusoidal signal (see Fig. 7). Within each subplot, the amplitude $A(\text{UT1-UTC})$ is depicted on the right while the left side is not populated. In the first column the reference station is located at -30 degrees latitude, in the second column at 0 degrees and in the third column at

50 degrees. In the first row of plots, (a) an error of $162 \mu\text{s}$ is introduced in the dX -component of the a priori nutation information, whereas the second row (b) shows the effect induced by the same error in the dY -component. Bilinear interpolations between the grid cells have been used to generate these plots

in general strongly affected by errors in the a priori polar motion.

Furthermore, again east–west-oriented baselines between any reference station and stations at the low- to mid-latitudes including δlon of over 120 degrees show no to little differences in the simulated UT1-UTC values and thus are relatively resistant against erroneous a priori information in the polar motion.

In comparison with the findings of Nothnagel and Schnell (2008) and Schartner et al. (2021), which are based on the partial derivatives of the polar motion components with respect to UT1-UTC , our simulations reveal why more sophisticated studies are necessary to investigate the impact of errors on the performance of UT1-UTC measurements. An evaluation based on the partial derivatives suggested that baselines with big differences in the z coordinates and north–south-oriented baselines are most affected by errors in the polar motion, whereas perfect east–west-oriented baselines including equatorial baselines are least affected. However, this is not reflected in our simulations. In the case of erroneous a priori polar motion, baselines located at the equator, with perfect east–west extension, result in a high variation of the monthly UT1-UTC differences (high $\sigma(\text{UT1-UTC})$ value), whereas baselines including a station in the low- to mid-latitudes show a small dependence and small variations.

Furthermore, just like in the case of errors in the north component of the topocentric coordinates of the remote antenna, the effects of errors in the polar motion are switched in sign for baselines mirrored at the equatorial plane. These findings imply that UT1-UTC from only northern hemisphere baselines can be biased through the introduction of inaccurate a priori polar motion or station coordinates and they point out the importance of southern *Intensive* baselines as a counterbalance.

3.3 Errors in nutation components

Since the effect of erroneous a priori nutation information on UT1-UTC strongly depends on the sidereal time, the simulation results cannot be combined to one bias $m(\text{UT1-UTC})$ and one standard deviation $\sigma(\text{UT1-UTC})$ per baseline. We note that the impact of both nutation components reveals a sinusoidal behavior with an annual period, thus confirming the results of Nothnagel and Schnell (2008). Therefore, to get a global picture, the amplitudes $A(\text{UT1-UTC})$ of the sinusoidal signal throughout the year induced by errors in the nutation offsets are calculated and displayed in Fig. 5. Again, the first row (5a) shows the results of the evaluation with an erroneous dX -component, whereas the second row (5b) the results of the evaluation where the dY -component is modified. In both cases, approximately 83% of baselines lead

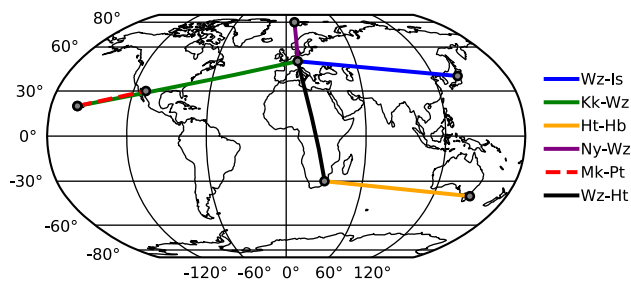


Fig. 6 Sketch of the six representative baselines

to amplitudes of over $5 \mu\text{s}$ and 35% of over $20 \mu\text{s}$. In general, it can be said that the greater the amplitude, the larger the variations implying a lower resistance against errors in the nutation offsets. For example, baselines with a midpoint close to the equatorial plane, especially baselines which are close to being parallel to the Earth's rotation vector, are most affected by errors in the nutation offsets. In contrast, short baselines and east–west baselines between any reference station and a station at low- to mid-latitudes including a δlon of over 120 degrees perform well.

To show the impact on UT1–UTC over the year, the results of six representative *Intensive* baselines (see Fig. 6) are displayed in Fig. 7, where the first row (7a) shows the effect of erroneous dX and the second row (7b) of erroneous dY information on the determination of UT1–UTC. In this case, the influence of errors in the a priori information in terms of value and sign strongly depends on the sidereal time and of course the geometry of the network. In general, the impact of both nutation components reveals a sinusoidal behavior with an annual period, confirming thus the results of Nothnagel and Schnell (2008). Due to these strong variations in the monthly UT1–UTC differences of the different baselines, two plots per error source are shown with different limitations. The left plot shows the results of two northern *Intensive* sessions between Wz and Is (Ishioka, Japan) (blue) and Kk and Wz (green), one southern *Intensive* session between Ht (Hartrao, South Africa) and Hb (Hobart, Tasmania) (orange) (Böhm et al. 2022) and one short north–south-oriented baseline between Ny (NyAlesund, Norway) and Wz (purple). In the right plot, the results of a short baseline between Mk and Pt (red) and a long north–south baseline between Wz and Ht (black) are displayed. Please note that these results do not show the exact values for the individual baselines since the baselines are only approximated by using the corresponding nearest grid antennas. For example, in the case of the baseline Wz-Is the baseline between the reference station at 50 degrees (Wz: 49.15 degrees *lat*, 12.88 degrees *lon*) and the second station at 40 degrees latitude and 130 degrees δlon (Is: 36.21 degrees *lat*, 140.22 degrees *lon*) is investigated.

Comparing the results of the southern baseline (Ht-Hb) and the results of the two northern INT1 baselines (Wz-Is,

Kk-Wz) shown in Fig. 7, it appears that the baseline located on the southern hemisphere performs slightly worse. However, if we compare the results of two baselines with the exact same geometry but mirrored at the equatorial plane, the difference between the monthly UT1–UTC differences is close to zero meaning that southern *Intensives* do not provide significant disadvantages. Furthermore, the phase of the southern baseline is shifted in time concerning both nutation offsets. The results of the two north–south-oriented baselines Ny-Wz and Wz-Ht show that the longer the north–south-oriented baseline is and the more parallel it is to the Earth's rotation vector, the greater the influence of errors in the nutation components. To be more precise, the baseline Ny-Wz only varies from approximately -5 to $5 \mu\text{s}$, while the longer north–south baseline Wz-Ht leads to higher variations by the factor of 10. Furthermore, short baselines (Mk-Pt) are also more affected by errors in the nutation components than longer baselines (e.g., Wz-Kk).

3.4 Impact of errors in a priori information on representative *Intensive* baselines

In summary, Table 1 lists the different evaluation results in terms of bias $m(\text{UT1–UTC})$ and standard deviation $\sigma(\text{UT1–UTC})$ or amplitude $A(\text{UT1–UTC})$ for six representative baselines. It is evident that all baselines are resistant against errors in the up direction of the remote station, whereas the impact of errors in the horizontal components lead to higher $m(\text{UT1–UTC})$ biases. North–south-oriented baselines are strongly affected by errors in the east coordinate and more resistant against errors in the north-component. Concerning errors in the a priori polar motion and nutation data, the short baseline Mk-Pt and Wz-Ht, which is close to parallel to the Earth's rotation vector, are most affected.

4 Conclusions

Intensive baselines with their main goal of determining the highly variable parameter UT1–UTC are strongly affected by the geometry of the network, the source selection (see Schartner et al. 2021) and the quality of the a priori information. This study shows that different errors in the a priori information influence the performance of *Intensive* sessions differently. To get a global picture of the behavior of the performance of *Intensives* which are compromised with errors in the a priori data, over 270,000 simulated schedules are investigated.

As already examined by Nothnagel and Schnell (2008), due to the daily rotation of the Earth and annual revolution around the Sun, the source visibility and hence the source selection within the individual schedules changes throughout the year (see Sect. 2.1) resulting in variations in the UT1–

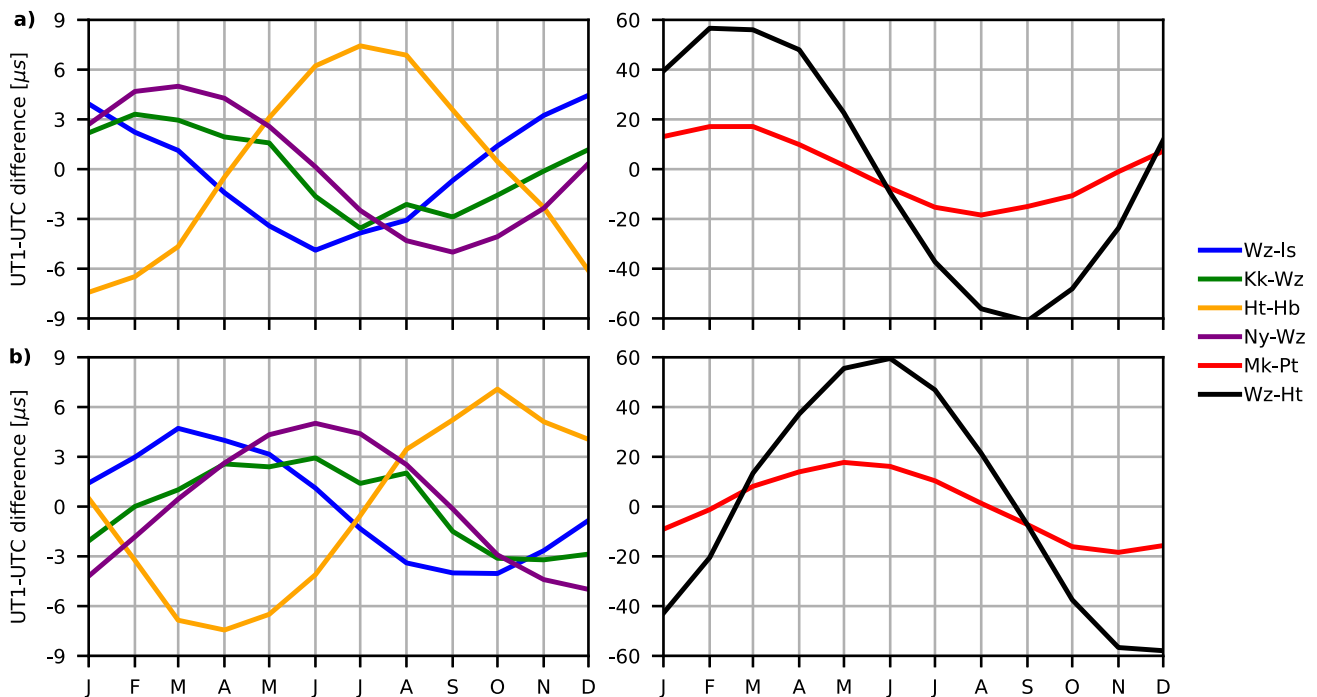


Fig. 7 Impact of erroneous a priori nutation data on the performance of *Intensive* sessions in terms of the monthly UT1–UTC differences plotted over the investigation period of one year. Note that due to these strong variations in the monthly UT1–UTC differences of the different baselines, two plots per error source are shown with different axis lim-

its. In the first row of plots (a) an error of 162 μs is introduced in the dX -component of the a priori nutation information, whereas the second row (b) shows the effect induced by the same error in the dY -component in the case of six selected *Intensive* sessions

Table 1 Impact of erroneous station coordinates in up, east and north direction and a priori polar motion in terms of bias $m(\text{UT1–UTC})$ and standard deviation $\sigma(\text{UT1–UTC})$ [μs] and impact of erroneous nutation

data in terms of the amplitude $A(\text{UT1–UTC})$ of the annual signal [μs] on the estimation of UT1–UTC concerning six representative *Intensive* baselines

Baseline	U [$\mu\text{s}/5\text{ mm}$]	E [$\mu\text{s}/5\text{ mm}$]	N [$\mu\text{s}/5\text{ mm}$]	x_p, y_p [$\mu\text{s}/229\ \mu\text{as}$]	$dXdY$ [$\mu\text{s}/229\ \mu\text{as}$]
Wz-Is	0.3 ± 0.4	-7.8 ± 0.2	-4.5 ± 0.2	5.3 ± 0.5	6.2
Kk-Wz	-0.1 ± 0.3	-6.8 ± 0.0	-1.1 ± 0.5	4.0 ± 0.9	4.6
Ht-Hb	0.2 ± 0.3	-6.2 ± 0.2	6.6 ± 0.6	-10.1 ± 0.9	10.9
Ny-Wz	-0.2 ± 0.5	-22.9 ± 0.0	0.7 ± 1.5	5.0 ± 0.3	6.9
Mk-Pt	1.5 ± 0.6	-0.9 ± 1.2	-26.5 ± 1.1	23.4 ± 1.4	26.0
Wz-Ht	0.7 ± 1.5	-47.2 ± 0.9	-5.0 ± 1.9	66.7 ± 0.6	85.4

The columns x_p, y_p and $dXdY$ represent the results from an evaluation where errors have been introduced in both x- and y-component of the polar motion and nutation offsets. Note that the induced error therefore no longer corresponds to the error introduced in the station coordinate components of 5 mm, but rather 7.1 mm or 229 μas

UTC differences ($\sigma(\text{UT1–UTC})$) of the monthly schedules. In addition to source visibility, the choice of sources within the scheduling process also plays a role, but this influence is smaller, as has been shown in Kern et al. (2023). In this study, great care is taken to provide highly optimized schedules by generating a compact list of suitable sources and ensuring the scheduling of corner observations. However, the impact of changes in the source selection is still visible in the variability of the UT1–UTC differences throughout the year ($\sigma(\text{UT1–UTC})$).

In Schartner et al. (2021), we suggested that very short and very long baselines as well as baselines with a midpoint close to the equatorial plane, including equatorial baselines, perform poorly. This behavior can be partly explained by the geometry of these baselines and the resulting lack in the variety of observed sources, affecting the variability of the partial derivative of the group delay τ with respect to UT1–UTC. In this study, these exact baselines are strongly affected by errors in the corresponding a priori information as well. In contrast, east–west-oriented baselines, besides equatorial

baselines, are more resistant against errors in the station coordinates, a priori polar motion and nutation information.

In general, introducing an error of 5 mm in the up coordinate of one antenna only slightly affects the performance of *Intensive* sessions (Fig. 3a) compared to errors in the horizontal components (Fig. 3b,c) where 65–85% of the baselines result in an absolute $m(\text{UT1-UTC})$ value of over $5 \mu\text{s}$ and about 19% of over $20 \mu\text{s}$. Furthermore, errors in the east direction have a strong influence on north–south-oriented baselines just like errors in the a priori polar motion information and in the nutation making them in general less suitable for UT1–UTC observations.

In the case of erroneous a priori polar motion (see Fig. 4a, b), in particular baselines with a midpoint close to the equatorial plane result in a high scatter of monthly UT1–UTC differences in the order of up to several tens of μs , whereas baselines including a station in the low to mid-latitudes show a small dependence and variation.

Overall, this study reveals that the impact of errors in the a priori polar motion information cannot be evaluated using the partial derivatives of the individual parameters with respect to UT1–UTC since it would suggest that equatorial baselines are least affected by errors in the polar motion and that a big difference in the baseline z coordinate is essential to reduce the impact of errors.

Concerning errors in the nutation components (Figs. 5a, b and 7a, b), it is shown that their impact strongly depends on the sidereal time resulting in a high variability of the UT1–UTC differences between the monthly schedules. Overall, baselines with a midpoint close to the equatorial plane, especially baselines oriented in north–south direction, are most affected by errors in both nutation offsets, whereas east–west baselines between a station and another station at mid- to high latitudes including a δlon of over 120 degrees are more resistant. For example, north–south baselines close to being parallel to the Earth’s rotation vector, like the baseline between Wz and Ht (Fig. 7a,b), lead to a high variability throughout the investigation period compared to short north–south baselines (e.g., Ny–Wz) with a maximum impact of about $\pm 5 \mu\text{s}$ compared to almost $\pm 60 \mu\text{s}$.

Comparing the results of the different reference stations in Figs. 3, 4, 5 and 7 it is evident that southern *Intensives* are as resistant against errors in the a priori information as sessions with stations located at the northern hemisphere and can even be used to mitigate systematics. For example, the currently observed southern Intensive session between Ht–Hb seems to be just as resistant against errors in the station coordinates, polar motion and nutation as the same baseline located on the northern hemisphere. Therefore, we suggest that observing southern *Intensives* provide no disadvantages and can be used to estimate UT1–UTC with a reasonable accuracy (for more information on southern *Intensives* and their performance see Böhm et al. (2022)).

As demonstrated in this paper, the contributions of different errors in the a priori information are not negligible since they have the same magnitude as the formal errors of the UT1–UTC estimates, which is between 5 and $20 \mu\text{s}$. This has to be taken into account when investigating the accuracy of the UT1–UTC estimations from *Intensive* sessions.

In our opinion, the results of this study show that the accuracy of predicted a priori EOP, used in the analysis of *Intensive* sessions, is crucial for the precise determination of UT1. Furthermore, the accuracy of the terrestrial reference frame (TRF) can significantly impact the UT1 estimate as well as uncorrected tropospheric signals which propagate into station coordinates and therefore impair the performance of *Intensives*. Thus, we suggest to rigorously use the newest EOP series (and predictions (Shahvandi et al. 2022)) and coordinates. In this case, a regular determination of updated TRF solutions (e.g., monthly TRF updates (Gross et al. 2022)) can be beneficial.

Acknowledgements The constructive comments and suggestions of four anonymous reviewers, which contributed significantly to the quality of the article, are highly appreciated. The authors acknowledge TU Wien Bibliothek for financial support through its Open Access Funding Programme. JB is grateful to the Austrian Science Fund (FWF) for funding project VGOS Squared (P 31625).

Author Contributions JB, LK and MS designed the study. LK performed the evaluations and analysis with help of SB and MS. All authors worked on the theoretical considerations, discussed the results and contributed on the final manuscript.

Funding Open access funding provided by Austrian Science Fund (FWF).

Data availability The datasets generated during and/or analyzed during the current study are publicly available at <https://doi.org/10.48436/08qqz-ymp66>. The software that was used to generate the results is publicly available at <https://github.com/TUW-VieVS/VLBI> and <https://github.com/TUW-VieVS/VieSchedpp>.

Declarations

Conflict of interest The authors declare that they have no conflict of interest.

Open Access This article is licensed under a Creative Commons Attribution 4.0 International License, which permits use, sharing, adaptation, distribution and reproduction in any medium or format, as long as you give appropriate credit to the original author(s) and the source, provide a link to the Creative Commons licence, and indicate if changes were made. The images or other third party material in this article are included in the article’s Creative Commons licence, unless indicated otherwise in a credit line to the material. If material is not included in the article’s Creative Commons licence and your intended use is not permitted by statutory regulation or exceeds the permitted use, you will need to obtain permission directly from the copyright holder. To view a copy of this licence, visit <http://creativecommons.org/licenses/by/4.0/>.

References

- Altamimi Z, Rebischung P, Métivier L et al (2016) ITRF2014: a new release of the international terrestrial reference frame modeling nonlinear station motions. *J Geophys Res Solid Earth* 121(8):6109–6131. <https://doi.org/10.1002/2016JB013098>
- Artz T, Leek J, Nothnagel A, et al (2012) VLBI intensive sessions revisited. In: Behrend D, Baver KD (eds) International VLBI service for geodesy and astrometry 2012 general meeting proceedings, pp 276–280
- Baver K, Gipson J (2014) Balancing sky coverage and source strength in the improvement of the IVS-INT01 sessions. In: Behrend D, Baver KD, Armstrong KL (eds) International VLBI service for geodesy and astrometry 2014 general meeting proceedings, pp 267–271
- Baver K, Gipson J (2020) Balancing source strength and sky coverage in IVS-INT01 scheduling. *J Geodesy* 94(2):18. <https://doi.org/10.1007/s00190-020-01343-1>
- Böhm J, Schuh H (2007) Forecasting data of the troposphere used for IVS intensive sessions. In: Proceedings of the 18th meeting of the European VLBI group for geodesy and astronomy, pp 153–157
- Böhm J, Hobiger T, Ichikawa R et al (2010) Asymmetric tropospheric delays from numerical weather models for UT1 determination from VLBI Intensive sessions on the baseline Wettzell-Tsukuba. *J Geodesy* 84:319–325. <https://doi.org/10.1007/s00190-010-0370-x>
- Böhm J, Böhm S, Boisits J et al (2018) Vienna VLBI and satellite software (VieVS) for geodesy and astrometry. *Publ Astron Soc Pac* 130(986):aaa22b. <https://doi.org/10.1088/1538-3873/aaa22b>
- Böhm S, Böhm J, Gruber J et al (2022) Probing a southern hemisphere VLBI intensive baseline configuration for UT1 determination. *Earth Planets Space* 74(118):1–16. <https://doi.org/10.1186/s40623-022-01671-w>
- Charlot P, Jacobs CS, Gordon D et al (2020) The third realization of the International Celestial Reference Frame by very long baseline interferometry. *Astron Astrophys* 644:A159. <https://doi.org/10.1051/0004-6361/202038368>
- Corbin A, Niedermann B, Nothnagel A et al (2020) Combinatorial optimization applied to VLBI scheduling. *J Geod* 94(2):19. <https://doi.org/10.1007/s00190-020-01348-w>
- Diamantidis PK, Haas R, Varenus E et al (2022) Combining VGOS, legacy S/X and GNSS for the determination of UT1. *J Geod* 96:55. <https://doi.org/10.1007/s00190-022-01648-3>
- Dieck C, Johnson M, MacMillan D (2023) The importance of co-located VLBI Intensive stations and GNSS receivers. *J Geod* 97:21. <https://doi.org/10.1007/s00190-022-01690-1>
- Gipson J, Baver K (2015) Minimization of the UT1 formal error through a minimization algorithm. In: Proceedings of the 22nd meeting of the European VLBI group for geodesy and astronomy, http://www.oan.es/raege/evga2015/EVGA2015_proceedings.pdf
- Gipson J, Baver K (2016) Improvement of the IVS-INT01 sessions through Bayesian estimation. In: Behrend D, Baver KD, Armstrong KL (eds) International VLBI service for geodesy and astrometry 2016 general meeting proceedings, pp 229–233
- Gross RS, Abbondanza C, Chin M, et al (2022) A sequential estimation approach to determining and updating terrestrial reference frames. Presented at the AGU Fall Meeting 2022, Chicago IL & Online Everywhere
- Hefty J, Gontier AM (1997) Sensitivity of UT1 determined by single-baseline VLBI to atmospheric delay model, terrestrial and celestial reference frames. *J Geod* 71(5):253–261. <https://doi.org/10.1007/s001900050093>
- Kareinen N, Klopotek G, Hobiger T et al (2017) Identifying optimal tag-along station locations for improving VLBI intensive sessions. *Earth Planets Space* 69(1):1–9. <https://doi.org/10.1186/s40623-017-0601-y>
- Kern L, Schartner M, Böhm J, et al (2023) Impact of the Source Selection and Scheduling Optimization on the Estimation of UT1-UTC in VLBI Intensive Sessions. In: Armstrong KL, Behrend D, Baver KD (eds) International VLBI service for geodesy and astrometry 2023 general meeting proceedings
- Krasna H, Malkin Z, Böhm J (2015) Non-linear VLBI station motions and their impact on the celestial reference frame and Earth orientation parameters. *J Geod* 89(10):1019–1033. <https://doi.org/10.1007/s00190-015-0830-4>
- Landskron D, Böhm J (2019) Improving dUT1 from VLBI intensive sessions with GRAD gradients and ray-traced delays. *Adv Space Res* 63(11):3429–3435. <https://doi.org/10.1016/j.asr.2019.03.041>
- Leek J, Artz T, Nothnagel A (2015) Optimized scheduling of VLBI UT1 intensive sessions for twin telescopes employing impact factor analysis. *J Geod* 89(9):911–924. <https://doi.org/10.1007/s00190-015-0823-3>
- Malkin Z (2011) The impact of celestial pole offset modelling on VLBI UT1 intensive results. *J Geod* 85(9):617–622. <https://doi.org/10.1007/s00190-011-0468-9>
- Malkin Z (2013) Impact of seasonal station motions on VLBI UT1 intensive results. *J Geod* 87(6):505–514. <https://doi.org/10.1007/s00190-013-0624-5>
- Niell A, Barrett J, Burns A et al (2018) Demonstration of a broadband very long baseline interferometer system: a new instrument for high-precision space geodesy. *Radio Sci* 53:1269–1291. <https://doi.org/10.1029/2018RS006617>
- Nilsson T, Soja B, Balidakis K et al (2017) Improving the modeling of the atmospheric delay in the data analysis of the Intensive VLBI sessions and the impact on the UT1 estimates. *J Geod* 91:857–866. <https://doi.org/10.1007/s00190-016-0985-7>
- Nothnagel A, Campbell J (1991) Polar motion observed by daily VLBI measurements. In: Proceedings of the AGU Chapman Conference on Geodetic VLBI: Monitoring Global Change; NOAA Technical Report NOS 137 NGS 49, Washington D.C., USA, pp 345–354
- Nothnagel A, Schnell D (2008) The impact of errors in polar motion and nutation on UT1 determinations from VLBI Intensive observations. *J Geod* 82(12):863–869. <https://doi.org/10.1007/s00190-008-0212-2>
- Nothnagel A, Artz T, Behrend D et al (2017) International VLBI service for geodesy and astrometry—delivering high-quality products and embarking on observations of the next generation. *J Geod* 91:711–721. <https://doi.org/10.1007/s00190-016-0950-5>
- Petit G, Luzum B (2010) IERS Conventions 2010. IERS Technical Note 36
- Petrachenko WT, Niell AE, Corey BE et al (2012) VLBI2010: next generation VLBI system for geodesy and astrometry. In: Kenyon S, Pacino MC, Marti U (eds) Geodesy for planet earth. Springer Berlin Heidelberg, Berlin, pp 999–1005
- Plank L, Lovell JE, Shabala SS et al (2015) Challenges for geodetic VLBI in the southern hemisphere. *Adv Space Res* 56(2):304–313. <https://doi.org/10.1016/j.asr.2015.04.022>
- Schartner M, Böhm J (2019) VieSched++: a new VLBI scheduling software for geodesy and astrometry. *Publ Astron Soc Pac* 131(1002):084,501. <https://doi.org/10.1088/1538-3873/ab1820>
- Schartner M, Böhm J, Nothnagel A (2020) Optimal antenna locations of the VLBI Global Observing System for the estimation of Earth orientation parameters. *Earth Planets Space* 72(1):87. <https://doi.org/10.1186/s40623-020-01214-1>
- Schartner M, Kern L, Nothnagel A et al (2021) Optimal VLBI baseline geometry for UT1-UTC Intensive observations. *J Geod* 95:75. <https://doi.org/10.1007/s00190-021-01530-8>
- Shahvandi MK, Schartner M, Soja B (2022) Neural ode differential learning and its application in polar motion prediction. *J Geophys Res Solid Earth* 127(11):e2022JB024775. <https://doi.org/10.1029/2022JB024775>

- Teke K, Böhm J, Madzak M et al (2015) Gns zenith delays and gradients in the analysis of vlbi intensive sessions. *Adv Space Res* 56:1667–1676. <https://doi.org/10.1016/j.asr.2015.07.032>
- Titov O (2000) Influence of adopted nutation model on vlbi neos-intensives analysis. *Int Astron Union Colloq* 180:5. <https://doi.org/10.1017/S0252921100000385>
- Uunila M, Nothnagel A, Leek J (2012) Influence of Source Constellations on UT1 Derived from IVS INT1 Sessions. In: Behrend D, Baver KD (eds) *International VLBI service for geodesy and astrometry 2012 general meeting proceedings*, pp 395–399, <https://ivscc.gsfc.nasa.gov/publications/gm2012/IVS-2012-General-Meeting-Proceedings.pdf>
- Wang J, Ge M, Glaser S et al (2022) Impact of tropospheric ties on UT1-UTC in GNSS and VLBI integrated solution of intensive sessions. *J Geophys Res Solid Earth* 127(11):e2022JB025228. <https://doi.org/10.1029/2022JB025228>
- Xu MH, Savolainen T, Zubko N et al (2021) Imaging VGOS observations and investigating source structure effects. *J Geophys Res Solid Earth* 126(4):e2020JB021238. <https://doi.org/10.1029/2020JB021238>
- Xu MH, Savolainen T, Anderson JM et al (2022) Impact of the image alignment over frequency for the VLBI Global Observing System. *Astron Astrophys* 663:A83. <https://doi.org/10.1051/0004-6361/202140840>